

An automated ac-magnetic susceptibility apparatus

A CHAKRAVARTI, R RANGANATHAN and A K RAYCHAUDHURI

Saha Institute of Nuclear Physics, 92 APC Road, Calcutta 700009, India

MS received 21 April 1990; revised 11 August 1990

Abstract. We report here both hardware and software for an ac susceptibility measurement system, namely the design and construction of the cryostat, coil system, sample rod assembly and also the automation of the sample rod movement, bridge control and nulling etc with the help of an inexpensive Z-80A microprocessor via a home-made IEEE-488 interface. The variable parameters are temperature, magnitude of the rms field and frequency. An entirely new dynamic bridge nulling algorithm with continuous sample movement, which eliminates to a large extent problems related to time-dependent drifts, has been developed. We also present some experimental data collected with this system.

Keywords. AC susceptibility; cryostat; mutual inductance bridge; automation; microprocessor.

PACS Nos 07-55; 75-30

1. Introduction

AC susceptibility (ACS) is an important experimental tool for measuring the magnetic and electronic properties of materials. This technique can be employed for studying magnetic transitions, spin-glass transitions, superconducting transitions, co-existence of magnetism and superconductivity, re-entrant spin-glass behaviour and dissipative processes related with finite relaxation times (from the complex susceptibility $\chi = \chi' + i\chi''$). Although a number of papers have appeared regarding the instrumentation aspects (van de Klundert *et al* 1975; Maxwell 1975; Corson 1982; Ranganathan and Rangarajan 1982; Martin and Wieser 1985; Ocio and Hamman 1985; Ramakrishnan *et al* 1985; Deutz *et al* 1989), certain specific practical details are generally lacking. In this paper we emphasize the following: (i) details for the construction of an inexpensive sample rod to minimize eddy currents and hence allow the accurate measurement of the imaginary component, χ'' of the susceptibility; (ii) a method for the accurate determination of the temperature at the actual sample site, as generally the sensor is located far away from the sample; (iii) an algorithm for the virtual elimination of drift problems arising due to temperature instability in the system, time-dependent drift in the bridge electronics and minute deformations in the coil configuration. The principle of the method is as follows: The sample under investigation forms the core of a transformer arrangement consisting of a primary and a pair of secondaries wound in opposition to each other to form a gradiometer configuration. By moving the sample between the two secondaries (corresponding to the mutual inductances M_{\downarrow} and M_{\uparrow}) the change in mutual inductance ΔM is measured and the susceptibility χ is found from $\chi = K\Delta M$ where K is a calibration constant which depends on the particular experimental arrangement. Thus the general procedure is

to calibrate the system with a well-known paramagnetic sample like Gd_2O_3 (Muly and Muly 1974), Mohrs salt (Martin 1967) etc. and then find the constant K .

2. Experimental system

2.1 Cryostat

Figure 1 shows the details of the cryostat (not to scale). The coil assembly and sample rod are enclosed in a thin-walled stainless-steel tube ($L = 980$ mm, $\phi = 38.2$ mm) which forms the exchange gas space of the cryostat. The wall of this outer tube is cooled by direct contact with the coolant (liquid nitrogen or helium as the case may be). A pumping port for the cryogen is provided in the main flange of the cryostat, and by reducing the pressure it is possible to achieve temperatures lower than the boiling point of the coolant. The sample rod and the coil assembly are cooled by allowing

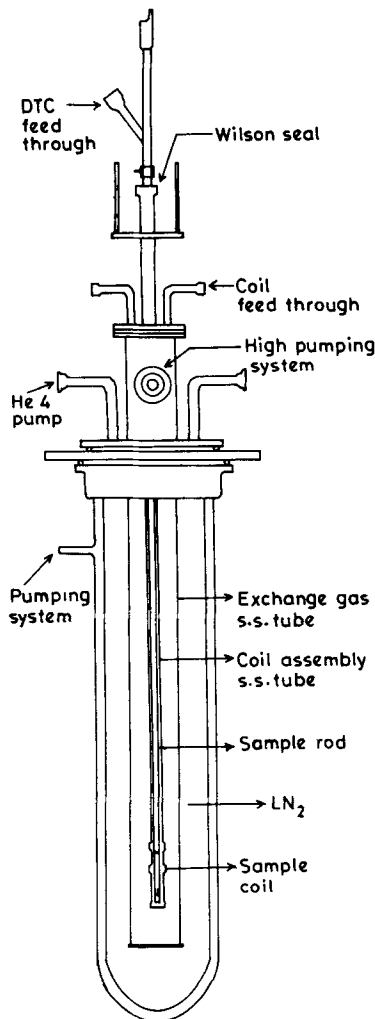


Figure 1. Cryostat details.

helium exchange gas into the exchange gas space, thus placing the sample in thermal contact with the cryogen. To stabilize the temperature, the exchange gas is pumped out to a high vacuum and by supplying a small current to a heating coil on the sample tube, the required temperature can be attained.

2.2 Coil system

The coil system is suspended inside the exchange gas space, without touching the walls, by means of a ss tube ($L = 954$ mm, $\phi = 12.7$ mm) which contains a threaded copper block at the lower end for mounting the coil formers. Radiation shields are provided at the outside of this tube to reduce heat radiation on to the coil system. The coil system consists of a primary of about 1500 turns of SWG 42 insulated copper wire. 50 additional turns are wound at each end of the solenoid to reduce fringe effects and make the field inside the primary uniform. Each of the secondaries are of about 2000 turns of insulated SWG 46 copper wire separated by a distance of about 10 mm. They are wound in the same direction but connected in series opposition. Special care has been taken to select the former of the coils so that the effect of thermal contraction and eddy current is minimum. The primary former is made out of low temperature epoxy from Oxford instruments, which has a very low coefficient of thermal expansion. This ensures a constant ac field inside the primary at all temperatures. The secondary is made of teflon. However, we believe that the performance of the system can be improved by making the secondaries with low thermal expansion coefficient materials. In order to reduce the temperature gradient along the length of the coil system and also to allow rapid dissipation of the $i^2 R$ heat generated in the primary due to the energizing current I_p , thermal link is established between the copper block and the coil system by enclosing the latter in a sheath made of insulated copper wires, which extends right up to the copper block and is secured to the coil assembly by thermally conducting GE7031 varnish. The primary coil is placed over the secondaries in order to increase the filling factor of the sample by keeping the secondaries as close to the sample as possible. The primary former is threaded with the secondary former for convenience. A Faraday shield, in the form of a single layer of tightly wound insulated copper wire with one end left floating and the other end grounded, is placed below the primary winding in order to reduce the capacitance between the primary and secondary. The mutual inductance between the primary and each of the secondaries is about 3 mH and the two secondaries have been balanced out to about $4 \mu\text{H}$ at room temperature, which goes up to about $20 \mu\text{H}$ at liquid nitrogen temperature. The present coil system can operate satisfactorily up to about 20 kHz with a current of 10 mA. The characteristics of our coil system is given in table 1. For a primary current of 10 mA, the field at the centre $\approx 4 \text{ Oe}$ (H_{rms}).

Table 1. Coil system details.

Quantity	Unit	Primary	Secondary 1	Secondary 2
Copper wire dia.	SWG	42	46	46
Length	mm	55	8	8
No. of turns		1500 + 50 + 50	2000	1951
Room temperature resistance	Ω	168	180	175

2.3 Sample rod

Figure 2 shows the details of the sample rod. At the top we have a steel tube ($L = 395$ mm, $\phi = 6$ mm) with arrangements for attachment with the stepping motor assembly. This steel tube is introduced into the coil ss tube through a Wilson seal, which ensures that a high vacuum can be maintained inside the cryostat even when the sample rod is being moved up and down. A long ss tube ($L = 803$ mm, $\phi = 4.5$ mm) is attached to this steel tube, at the end of which is a small copper block acting as a cold reservoir with grooves for mounting a diode temperature sensor and a heating coil (RT resistance = 67.2Ω). In order to reduce eddy current effects, the sample is mounted on a tube made out of a bundle of copper wires ($L = 101$ mm, $\phi = 4$ mm) which in turn is connected by soft soldering to the copper block. The copper block and thermometer, both of which would give a large signal, do not move into the coil system during any state of measurement. In order to reduce the signal due to the sample slot (Roy *et al* 1982) we did not remove any material from the sample site. The sample tube was deformed at the sample site in the form of a slot. This ensured that the same amount of copper wire is present in both the secondaries, causing a further compensation in the empty sample rod contribution. We have found that this sample rod gives a negligible signal ($< 0.01 \mu\text{H}$) while providing relatively good

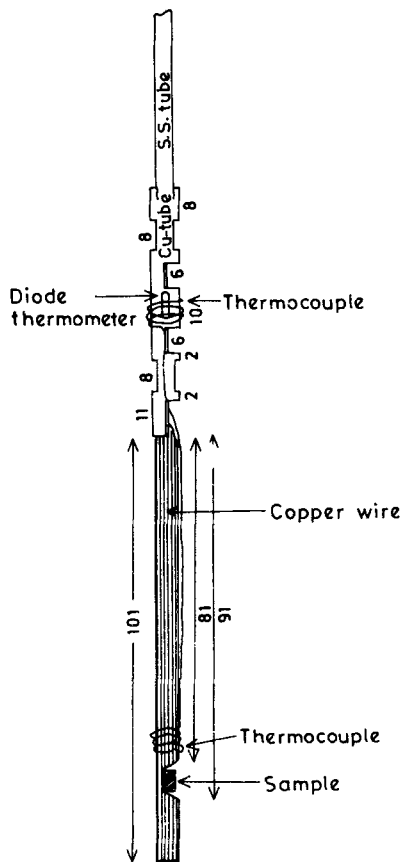


Figure 2. Sample rod details.

thermal contact between the block and the sample, and the eddy current is minimized.

Even though the copper wires have good thermal conductivity, due to the rather large distance between the thermometer and the sample (120 mm) a temperature difference is often developed between the two. The usual practice is to assume that this difference is a function of temperature only. A calibration of error versus temperature is then done using a known sample, and this error table is used to ascertain the sample temperature during all subsequent runs. We find this procedure unsatisfactory, because the error in temperature measurement is a function of the heat-loss from the sample, and this is not just a function of temperature alone; environmental factors like degree of vacuum, cryogen level, radiation onto the sample, etc. also have an appreciable effect. In order to measure the temperature of the sample in situ, we have used a Cr-FeAu-Cr differential thermocouple, (Lake Shore 0.07% Fe, Rosenbaum 1968) one junction of which is fixed to the copper block near the diode sensor as a reference temperature and the other end in the copper wires very near the sample. Adequate care has been taken to ensure good thermal anchoring of the thermocouple near the two ends with GE7031 varnish. The voltage across the thermocouple is measured with a nanovoltmeter (Keithley K181) and gives a direct measurement of the difference in temperature between the diode sensor and the sample. This ensures extremely accurate temperature determination, with an accuracy of the order of 0.1 K. However, the thermocouple has been found to give a small signal ($\approx 0.13 \mu\text{H}$) and our practice is to measure this signal by an empty sample rod run and then to subtract out this contribution from the actual signal. The temperature is controlled at the diode sensor site with the help of a Lake Shore model 520 temperature controller.

When the sample is moved up or down, an appreciable change occurs in the temperature of the sample. Since $M \uparrow$ and $M \downarrow$ should be measured at the same temperature, two procedures may be followed. By moving the sample repeatedly up and down a number of times the temperature fluctuation at the sample site may be minimized down to ~ 0.5 K or even lower. The values of $M \uparrow$ and $M \downarrow$ may then be recorded. In the other method (Deutz *et al* 1989) two curves are fitted to $M \downarrow$ and $M \uparrow$ in the neighbourhood of the temperature of interest. Then the values at that temperature may be computed to good accuracy by interpolation. The first method is useful if the error voltages from the lock-in amplifiers are recorded on a chart recorder without trying to balance out the bridge. However, the inherent inaccuracies of non-null-deflection methods cannot be avoided in this method. If the bridge has to be balanced out, normally the second method is the only option as some time is required to balance out the bridge and one has to wait till the sample temperature stabilizes to a new value. However, this method is very slow and there is another serious disadvantage. There may be large differences in time between measurements of corresponding $M \downarrow$ and $M \uparrow$ values and if some drift has taken place in the meantime, the accuracy will be reduced. We have been able to develop a procedure which has the advantages of both methods, allowing the bridge to be balanced even while the sample rod is being moved continuously up and down with an acceptably small resting period in each coil. The details are given in a later section. The accuracy of temperature measurement was verified by measuring the ferromagnetic transition temperature of an amorphous ribbon of $\text{Ni}_{69.6}\text{Fe}_{10.4}\text{Si}_8\text{B}_{12}$, (wt. = 4 mg) and it was found that the measured $T_c \approx 159 \pm 0.5$ K was in good agreement with the reported value in literature (Ranganathan *et al* 1985; Thummes *et al* 1988).

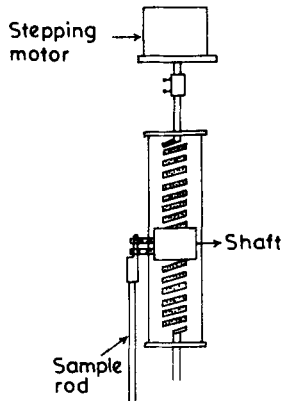


Figure 3. Sample rod movement assembly.

2.4 Sample movement assembly and stepping motor

In this type of experiment, the sample position has to be controlled with accuracy. This is because: (i) the primary cannot be made very long due to constraints of space and even after taking all precautions the field inside may not be that uniform. (ii) the secondaries have lengths comparable to the sample. As a result, fringe effects cause a large change if the sample is displaced along the axis. Thus any error in the sample position relative to the position of the secondaries will cause an error in the mutual inductance, particularly for larger samples.

In order to minimize this source of error, we have made an arrangement (figure 3) for moving the sample with the help of a microprocessor-controlled (Z-80) stepping motor (Rowley and Myers 1987). The top of the sample rod is attached to a nut which moves along a threaded shaft. This shaft is rotated by means of a stepping motor which can execute 1.8° steps. Since the pitch of the thread is ≈ 3.5 mm one step corresponds to ≈ 0.0175 mm. However, due to backlash errors, the accuracy is considerably reduced to about 0.1 mm. For controlling the stepper we have used the MFZ-16 microprocessor training kit, which uses the widely used and inexpensive microprocessor Z-80A from Zilog. A simple interface has been fabricated and the necessary software developed. The total number of steps that our programme can execute without modification is 2^{16} . To move the sample from one coil maximum to another, (a distance of ~ 20 mm), nearly 1200 steps have to be executed. The speed is variable and can be altered at will. A gradual acceleration algorithm has been used in order to prevent jerky movement which may result in steps being missed.

3. Calibration

The block diagram of the whole arrangement is shown in figure 4. The mutual inductance bridge from L'ATNE has a frequency range of 5 Hz to 50 kHz with a resolution of $0.01 \mu\text{H}$. There are two built-in phase sensitive detectors for the phase (M') and quadrature (M'') components. We have found that the unbalanced bridge output voltage is linear with the mutual inductance throughout the gain range from

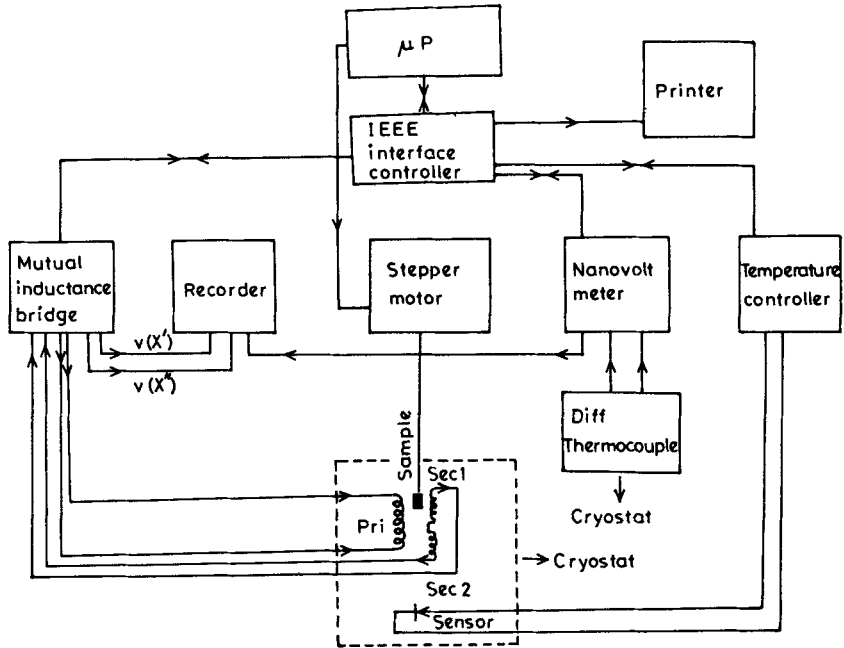


Figure 4. Block diagram for the whole set up.

0.1 to 100, and obey the relations:

$$V'(\text{mV}) = 2.461 \times \text{gain} \times I_p(\text{mA}) \times M'(\mu\text{H}). \quad (1a)$$

$$V''(\text{mV}) = 0.8896 \times \text{gain} \times I_p(\text{mA}) \times M''(\mu\text{H}). \quad (1b)$$

Thus, for a gain of 100 and primary current $I_p = 10 \text{ mA}$, $1 \mu\text{H}$ corresponds to 2461 mV in the M' channel and 889.6 mV in the M'' channel. By using a chart recorder and Keithley 181 nanovoltmeter, it is possible to measure mutual inductance directly from the voltage to an accuracy of $\approx 0.05 \mu\text{H}$, for typical values of $10 \mu\text{H}$.

In order to calibrate our system, we have taken a standard Gd_2O_3 (Mulay and Mulay 1974) sample of weight 92.2 mg. The temperature was controlled to an accuracy of $\approx 0.5 \text{ K}$ using a calibrated Si diode from Scientific Instruments. The sample temperature was measured using the differential thermocouple to an accuracy of 0.1 K using Keithley 181 nanovoltmeter. After stabilizing the temperature, the sample was moved up and down a few times by the stepping motor/ μP arrangement and the change in voltage recorded by the chart recorder.

The susceptibility of Gd_2O_3 is given by

$$\chi(T) = \frac{0.04524}{T + 17.5} \text{ emu/gm}. \quad (2)$$

We found that the χ'' component is negligible at the low frequency of 433 Hz i.e. $\chi' \rightarrow \chi$, the static susceptibility. A linear fit of $(\Delta M')^{-1}$ versus T gives the intercept -17.4 K which is in good agreement with the literature value of -17.5 K , (figure 5). On

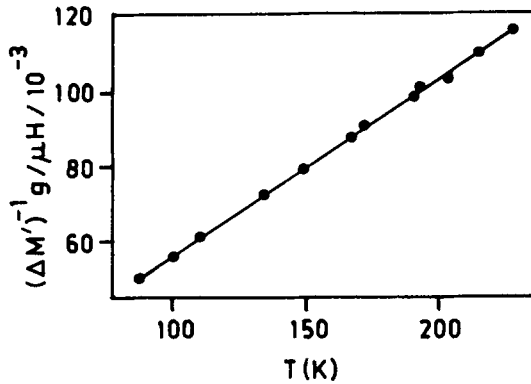


Figure 5. Calibration curve with Gd_2O_3 .

calculating the calibration constant K from the linear fit, we found that for our system:

$$K = 2.14 \times 10^{-5} \text{ emu}/\mu\text{H}. \quad (3)$$

The consistency of the calibration constant was checked by repeating the experiment with standard Mohr's salt where $\chi = C/T$, $C = 9.6 \times 10^{-3}$ (Martin 1967) for about 69 mg of the substance. We have also given in figures 6 and 7 some of the experimental results using this set up for the typical ferromagnetic transition of $Au_{75}(FeNi)_{25}$ (Chakravarti *et al* 1990), high T_c superconductor $Bi_xSr_2Ca_2Cu_4O_y$ ($x = 0.5, 1.0, 1.5$) (Chatterjee *et al* 1989) where χ' and χ'' have been measured in the vicinity of T_c with different ac fields.

4. IEEE-488 interface and bridge nulling algorithm

The mutual inductance bridge that we use (from L'ATNE, France) is equipped with an IEEE-488 interface. Through this interface it is possible to: (i) change the gain of the bridge. (ii) change the settings on the M' and M'' channels. (iii) read the off-balance voltages from the M' and M'' lock-in amplifiers. The frequency, current and time constant parameters have to be set manually.

Since our microprocessor trainer is not equipped with an IEEE-488 controller, we have developed an interface and software for controlling other instruments capable of talking or listening on the IEEE bus. Two 'port' ICs have been used. Ports A and B of the intel 8255 programmable input/output device have been used to handle the bus management and handshake lines. Port B of the Z-80 PIO has been used for data transfer between the microprocessor and the other equipments. The handshake lines are buffered and the outputs are of the open-collector type for wired-OR operation with pull-up resistors. The IEEE-488 protocol has been implemented with the help of subroutines which double check the status of the handshake lines for protection against noise spikes. This slows down the data transfer to a large extent but increases reliability greatly.

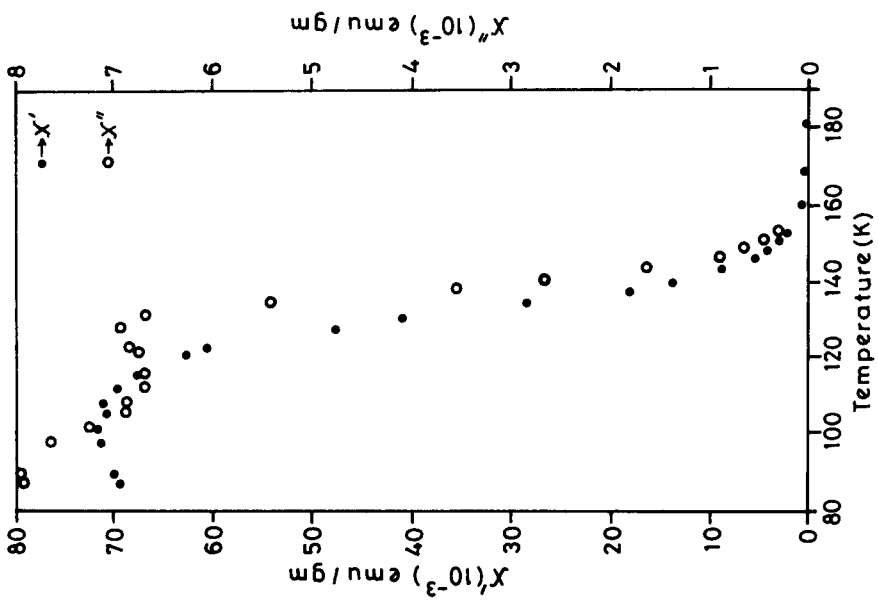


Figure 6. Ferromagnetic transition of $\text{Au}_{75}(\text{FeNi})_{25}$.

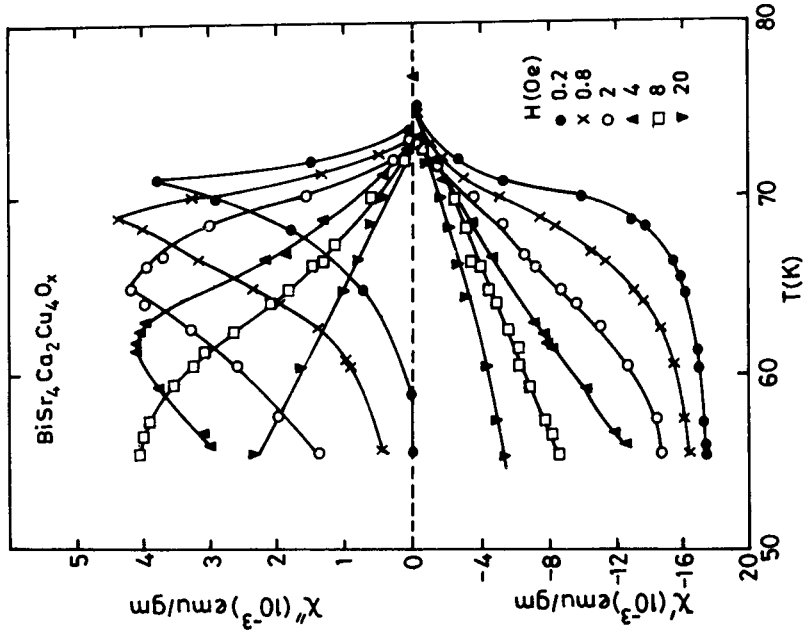


Figure 7. Superconducting transition of $\text{Bi}_x\text{Sr}_2\text{Ca}_2\text{Cu}_4\text{O}_y$.

The total measurement cycle goes as follows: (i) the bridge gain is set at zero. (ii) the sample is moved into the upper coil. (iii) previously calculated values of M' and M'' are output to the thumbwheel switches. (iv) final gain is read in from memory and output to the bridge. (v) the off-balance voltages in the two channels are read in. (vi) using equations 1a and 1b, the values of the mutual inductance of the two channels are modified and stored in memory. (vii) the value of the differential thermocouple voltage is read in from the nanovolt meter and stored in memory. (viii) the gain of the bridge is set at zero. (ix) the sample is moved into the lower coil. (x) an exactly similar procedure is followed here also. (xi) operation is repeated from step one onwards.

The main advantage of this algorithm* is that correction for the error in the previous step is made only after the sample has moved up and down once more. This drastically reduces the time during which the sample rod stays stationary in one coil, thus reducing the temperature change of the sample from coil to coil. Once locked, the algorithm is auto-tracking and the bridge remains balanced even if the temperature is changed slowly. Pressing the 'vector interrupt' key causes the main programme to branch to a subroutine which places the current values of mutual inductance and differential thermocouple voltages in a file which may then be accessed manually. This algorithm has been extremely successful and a resolution to the tune of $0.01 \mu\text{H}$ which corresponds to about 2×10^{-7} emu has been achieved. The bridge locks on to the correct values within a few minutes of starting.

5. Conclusion

An ac susceptometer has been assembled by incorporating a cryostat, sample rod and coil system. All the above hardware has been designed and constructed. The Z-80 microprocessor has been employed for sample movement control, bridge nulling, and data acquisition. The highlight of this work is the low cost of the experimental system and its high sensitivity; for example we have shown the applicability of an inexpensive microprocessor trainer as compared to a PC. The system has been calibrated in terms of paramagnetic materials, and ferromagnetic and superconducting transitions. Based on the calibration of the present experimental set-up with the standard sample, we found that $1 \mu\text{H} \approx 2.14 \times 10^{-5}$ emu with a resolution of $0.01 \mu\text{H}$. This sensitivity is comparable with the commercially available magnetometers, for example model 7000 ac susceptometer from Lake Shore Instruments (susceptibility sensitivity: 4×10^{-6} cgs units for typical ac field ~ 10 gauss) and EG&G, PARC vibrating sample magnetometer (magnetization sensitivity: 10^{-4} emu).

Acknowledgements

We thank Mr T K Pyne for his technical help, and Dr C D Mukherjee and Prof N Chatterjee for providing HTSC samples.

* Details of the hardware and software will be supplied by the authors on request.

References

- Chakravarti A, Ranganathan R, Raychaudhuri A K and Bansal C 1990 (To be communicated)
- Chatterjee N, Mukherjee C D, Ranganathan R, Chakravarti A and Raychaudhuri A K 1989 *Physica* **C161** 589
- Corson M R 1982 *Rev. Sci. Instrum.* **53** 1606
- Deutz A F, Hultsman R and Kranenberg F J 1989 *Rev. Sci. Instrum.* **60** 113
- Martin D H 1967 *Magnetism in solids* (Cambridge, Mass: MIT Press) p. 205
- Martin W E and Wieser J 1985 *J. Phys.* **E18** 342
- Maxwell E 1975 *Rev. Sci. Instrum* **36** 577
- Mulay L N and Mulay I L 1974 *Anna. Chem.* **46** 490R
- Ocio M and Hamman J 1985 *Rev. Sci. Instrum.* **56** 1367
- Ramakrishnan S, Sundaram S, Pandit R S and Girish Chandra 1985 *J. Phys.* **E18** 650
- Ranganathan R and Rangarajan G 1982 *Pramana – J. Phys.* **19** 65
- Ranganathan R, Tholence J L, Krishnan R and Dancygier M 1985 *J. Phys.* **C18** 1057
- Rosenbaum R 1968 *Rev. Sci. Instrum.* **39** 6
- Rowley A T and Myers A 1987 *J. Phys.* **E20** 146
- Roy A, Scott B D, Ginsberg D M and Roach P R 1982 *Rev. Sci. Instrum.* **53** 1053
- Thummes G, Kotzler J, Ranganathan R and Krishnan R 1988 *Z. Phys.* **B69** 489
- van de Klundert L J M, de Rooij C, Caspari M, and von der Marel L C 1975 *Cryogenics* **15** 577